



Spatial analysis of remote sensing and meteorological indices in a drought event in southwestern Spain

Elia Quirós¹ · Laura Frago-Campón¹

Received: 2 November 2023 / Accepted: 11 January 2024 / Published online: 31 January 2024
© The Author(s) 2024

Abstract

The effects of global warming and climate change are being felt through more extreme and prolonged periods of drought. Multiple meteorological indices are used to measure drought, but they require hydrometeorological data; however, other indices measured by remote sensing and used to quantify vegetation vigor can be correlated with the former. This study investigated the correlation between both index types by vegetation type and season. The correlations were also spatially modeled in a drought event in southwestern Spain. In addition, three maps with different levels of detail in terms of vegetation categorization were compared. The results generally showed that grassland was the most well correlated category between the SPEI and the FAPAR, LAI, and NDVI. This correlation was more pronounced in autumn and spring, which is when most changes in vegetation senescence and growth occur. The spatiotemporal analysis indicated a very similar behavior for grasslands grouped in an area indicated by the climate change adaptation maps as having a high evapotranspiration forecast. Finally, in a forest-based forecast analysis, the indices that best explained the performance of the SPEI were again FAPAR, LAI, and NDVI, with a lag of up to 20 days. Therefore, the results showed that remotely sensed indices are good indicators of drought status and can be variably explanatory of traditional drought indicators. Moreover, complementing the study with spatiotemporal analysis made it possible to detect areas particularly vulnerable to climate change.

1 Introduction

Drought is a transitory, prolonged anomaly characterized by a period of below-normal precipitation values in a specific area. According to the American Meteorological Society (1997), drought can be classified into four interrelated categories over time (Tian et al. 2020; Yihdego et al. 2019). First, the initial cause of any drought is a shortage of precipitation (meteorological drought), leading to soil water deficiency that impacts crops when it occurs in the growing season (agricultural drought). After a prolonged period of no rainfall, there is a shortage of stream flow, groundwater recharge and reservoir volume (hydrological drought). Finally, the water resources needed to supply existing demand are affected (socioeconomic drought). Flash drought is a critical subseasonal phenomenon that can be devastating

for ecosystems and, consequently, for the economy and health in general (Christian et al. 2021).

Drought impacts are often assessed using drought indices that quantify the degree of drought hazard based on climate data (Vicente-Serrano et al. 2012). It is difficult to objectively quantify the characteristics of drought episodes in terms of intensity, magnitude, duration and spatial extent (Tian et al. 2020; Vicente-Serrano et al. 2012), and previous studies have shown that there is no single drought index with the ability to comprehensively assess water stress conditions in any type of bioclimatic variant (Cai et al. 2023; Yihdego et al. 2019). Even so, we can classify the indices into different groups: climate-based indices for assessing meteorological drought; remote sensing-based indices for vegetation analysis and soil-moisture-based indices mainly for assessing agricultural drought; hydrological-based indices for controlling stream flow alterations; and mixed-based indices, as a combination of the previous indices, since the different types of drought are interconnected (Abdourahmane et al. 2022). It has been shown that combining multiple variables and indices can improve drought characterizations (Liu et al. 2020). In either case, the calculation of drought indices requires the availability of hydrometeorological,

✉ Elia Quirós
equiros@unex.es

Laura Frago-Campón
laurafrago@unex.es

¹ Universidad de Extremadura, Escuela Politécnica, Avda. Universidad S/N, 10003 Cáceres, Spain

vegetation cover, crop productivity and flow regime data, depending on the type of drought to be monitored and the impacts to be assessed (Abdourahamane et al. 2022). These data come from in situ data-recording stations (weather stations and gauges) and from remote sensing data, which complement the previous data by increasing their spatiotemporal resolution and can be used in combination with in situ data or alone in regions with a lack of in situ data (Rhee et al. 2010; Xie and Fan 2021).

Within the climate-based group, several indices have been defined over the years, such as the Palmer drought severity index (PDSI) proposed by Palmer (1965), based on a soil water–balance equation. Subsequently, the widely used standardized precipitation index (SPI) (McKee et al. 1993), based on a probabilistic approach to precipitation, was defined. Finally, the standardized precipitation evapotranspiration index (SPEI) proposed by Vicente-Serrano et al. (2010) is a multiscale drought index based on climatic data. It can be used to determine the onset, duration, and magnitude of drought conditions relative to normal conditions.

In recent years, many studies have examined the relationship between different drought indices to identify the impacts of drought from different perspectives. For this purpose, the correlation between different climate-based drought indices (mostly PDSI, SPI, SPEI) and hydrological-, vegetation-, or agricultural productivity-based indices are usually analyzed (Abdourahamane et al. 2022; Alkaraki and Hazaymeh 2023; Cai et al. 2023; Kogan 1995b; Liu et al. 2020; Potop 2011; Rhee et al. 2010).

Nonetheless, with the integration of remote sensing data, new opportunities for drought monitoring have emerged by combining climate-based drought indices and satellite data with other biophysical parameters to determine negative impacts on vegetation (Yihdego et al. 2019). Regarding satellite data sources, remote sensing-based indices are frequently calculated using data from the Moderate Resolution Imaging Spectroradiometer Satellite (MODIS), mostly focused on products derived from the normalized difference vegetation index (NDVI) (Rouse et al. 1973), the most widely used index worldwide (Abdourahamane et al. 2022; Alkaraki and Hazaymeh 2023; Cai et al. 2023; Gu et al. 2007; Liu et al. 2020; Orimoloye et al. 2021; Rhee et al. 2010; Xie and Fan 2021). The MODIS instrument captures images of the earth every day or two. The extensive data products derived from MODIS observations describe characteristics of the land, oceans, and atmosphere that can be used to study both local and global scale phenomena and trends.

The information provided by the NDVI and its relationship with drought can be used directly or through other derived indices, such as the vegetation condition index (VCI) (Kogan 1995b) based on the NDVI or the vegetation

health index (VHI) (Kogan 1997), which is a mixed index combining the VCI with the temperature condition index (TCI) (Kogan 1995a). These products have been widely applied for detecting and monitoring drought since they are recommended by the World Meteorological Organization (WMO) (Xie and Fan 2021).

Another option is to work directly with the NDVI value. Recent studies such as Vicente-Serrano et al. (2019) have addressed the relationship between the NDVI and drought events. They concluded that although vegetation activity over large parts of Spain is closely related to the interannual variability of drought, there are clear seasonal differences in the response of the NDVI to drought. Thus, apart from the NDVI, there are other spectral indices that are useful for determining the negative effects of drought on vegetation. These are the dry matter productivity (DMP) (Monteith 1972), which represents the overall growth rate or increase in dry biomass of vegetation and is directly related to the net primary productivity of the ecosystem, and the fraction of absorbed photosynthetically active radiation (FAPAR), which quantifies the fraction of solar radiation absorbed by living leaves for photosynthetic activity. Additionally, the fraction of vegetation cover (Fcover), which refers only to the green and living elements of the canopy, corresponds to the fraction of soil covered by green vegetation. In practice, it quantifies the spatial extent of vegetation. Finally, the leaf area index (LAI) is defined as half the total area of green canopy elements per unit of horizontal soil surface. Some of these indices have been previously correlated with meteorological indices, such as the FAPAR (Gobron et al. 2005; Rossi et al. 2008;).

It should be noted that not all vegetation types behave in the same way during drought episodes. Moreover, there are few studies assessing the effects of drought by season, although seasonality and prevailing time scales can be relevant to assess drought impacts on different vegetation types (Vicente-Serrano et al. 2013). Therefore, a detailed study by vegetation type and season is needed to understand in detail the sometimes devastating effects of drought. If a spatial analysis can also be performed by grouping areas with the same performance, concise actions for economic aid or more focused actions for preventing the effects of climate change could be envisaged. This type of analysis would have important implications for characterizing priority intervention areas and informed decision-making to drive mitigation and adaptation efforts (Khoshnazar et al. 2023).

The main purpose of this work is to test the relationship, both temporally and spatially, between meteorological and remote sensing indicators in a drought event in southwestern Spain. To this end, we seek to answer the following questions: Is there a correlation between the indicators? Does the

correlation depend on vegetation type? Does the correlation depend on season? Can the correlation be spatially modeled?

2 Materials and method

2.1 Study area

The study area is the Extremadura region in western Spain (Fig. 1), which is covered mainly by forest and crops. Forested areas comprise evergreen forests, deciduous forests, shrubs, grasslands and dehesas. The dehesa is a typical cover of Extremadura and the neighboring border region with Portugal (where it is called montado) defined by Devesa Alcaraz (1995) as “pasturelands populated by holm and/or cork oaks, with an understory of open grassland, cereal crops, or Mediterranean scrub.”

The average annual precipitation of the area ranges from 400–1300 mm and is mainly concentrated in October–April, while during the summer, there is close to 0 mm of precipitation.

2.2 Indices

There are two different types of vegetation indices: radiometric indices, which are spectral transformations of two or more bands, and biophysical indices, which are based on radiative transfer models related to robust assumptions, mainly regarding canopy architecture (Huete et al. 2002).

The vegetation indices used in this work were downloaded from open access databases. The following vegetation indices from the Copernicus Global Land Service were used:

DMP: A biophysical index computed by the Monteith variant with a specific term that considers potentially important factors, such as the effect of droughts, nutrient deficiencies, pests and plant diseases. However, it can be argued that the adverse effects of disease and water or nutrient scarcity are manifested in the remotely sensed FAPAR term also used in the calculation of DMP.

FAPAR: A biophysical index dependent on the structure of the canopy, the optical properties of the vegetation elements and the lighting conditions (Smets and Lacaze 2019).

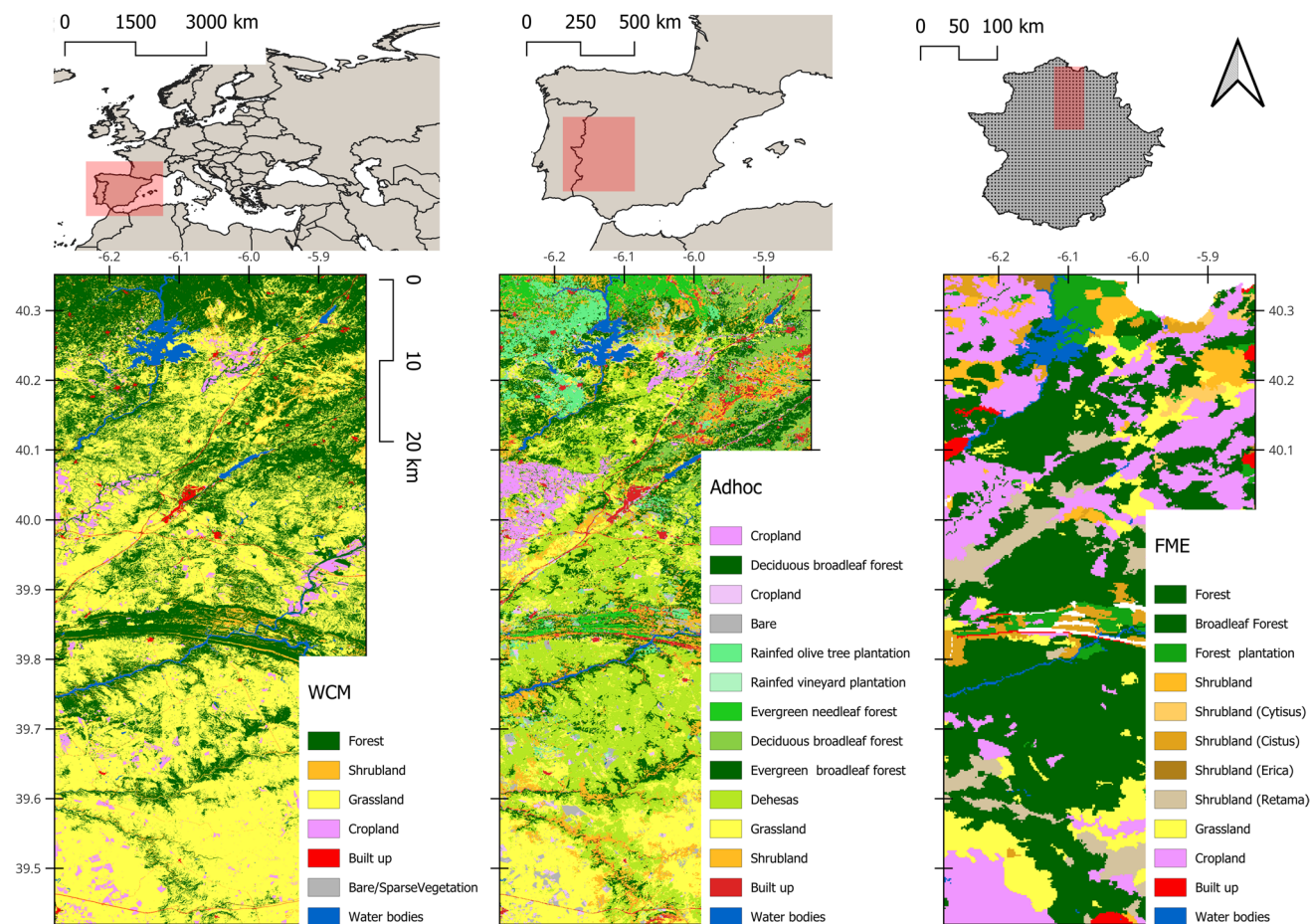


Fig. 1 Study area

The European Drought Observatory (European Commission 2023) uses the FAPAR anomaly to detect and monitor the impacts of agricultural drought on vegetation growth and productivity.

FCOVER: A biophysical index that corresponds to the gap fraction for the nadir direction. It is used to separate vegetation and soil in energy balance processes, including temperature and evapotranspiration. It is computed from the LAI and other canopy structural variables and does not depend on variables such as the geometry of illumination, in contrast to the FAPAR (Smets and Lacaze 2019). For estimation, only the green vegetation at both the overstorey and understorey levels will be considered.

Finally, the LAI serves to calculate the FCOVER and other indices and can therefore be considered a primary biophysical variable related to the canopy structure and is sensitive to droughts or other natural hazards (Delegido et al. 2015).

All indices that quantify green vegetation need to be calculated considering variables such as leaf water content, leaf dry matter content and leaf chlorophyll content (Weiss and Baret 2016), which are directly related to drought and are mainly related to dry or wet conditions.

Finally, the well-known NDVI is a spectral vegetation index that considers the fact that green and vigorous vegetation is reflected more in the NIR band and less in the visible part, making this index sensitive to drought.

The meteorological index SPEI was also obtained from the open database of the meteorological drought monitor of

the Spanish scientific research council (Reig et al. 2023). As noted above, this index identifies different drought types and impacts.

The SPEI uses the climatic water balance. It compares the available water with the atmospheric evaporative demand (Beguería et al. 2014). The climatic water balance is calculated at different time scales, and the results are fit to a log-logistic probability distribution.

Following the classification of Zhang et al. (2023), the severity of drought is classified by grading the SPEI as follows: no drought for values above -1, light drought for values between -1.5 and -1, moderate drought for values between -2 and -1.5, and severe drought for values below -2.

On the basis of all these data, the methodology followed is shown in Fig. 2.

2.3 Selection of study period and data collection

In terms of meteorological drought, historical precipitation time series were analyzed, and the period from October 2004 to October 2006 was selected. After limiting the study to this period of time, we downloaded all the abovementioned indices from the two databases in raster format and with a 1-km spatial resolution.

The vegetation indices were provided in 10-day periods and the SPEI in four-time steps per month, requiring the prior homogenization of the series to obtain equivalence for each period.

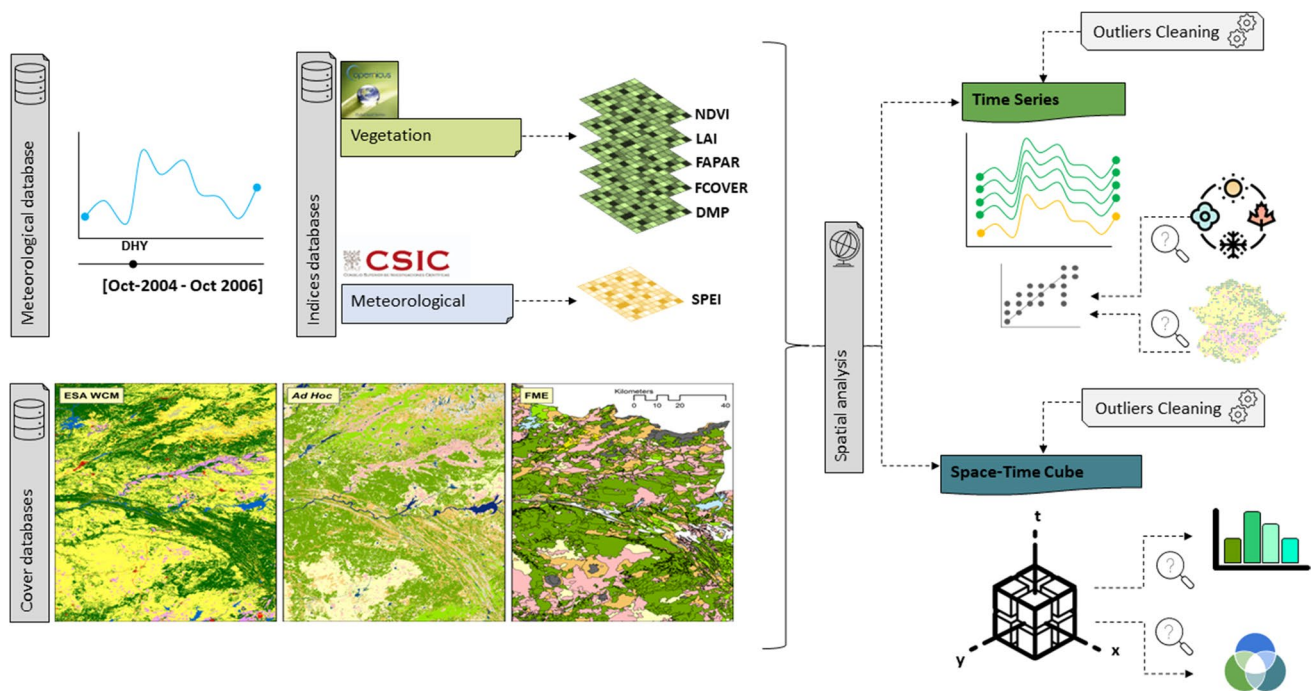


Fig. 2 Workflow

This resulted in a total of 360 rasters for the vegetation indices and 96 rasters for the drought index. The information was then extracted to a regular sample grid of locations regularly distributed throughout the study region. The distance between each position was 10 km, giving a total of 1737 locations to study.

2.4 Time series and correlation

A complete time series was generated with all 792,072 observations to establish correlations and comparisons between the evolution of the different vegetation indices and the SPEI. Using the severity degrees proposed by Zhang et al. (2023), we analyzed only the period with SPEI values below -1.0 (Fig. 2), which corresponds with a complete year from March 2005 to March 2006.

The time series were debugged by cleaning the outliers, such as pixels with digital levels of 255 or other atypical values.

Then, correlations were measured by Pearson's statistics and established according to two fundamental characteristics of the vegetation cover. First, a distinction was made between the different seasons of the year. Additionally, the correlations were investigated by vegetation type. For this purpose, three cartographic sources were used:

The ESA_WCM map, published on 24 October 2022 (Zanaga et al. 2022). This is a 10-m resolution cover map that distinguishes 11 categories, although we only worked with those that exclusively refer to the vegetation present in the study area.

The FME (Forest Map of Extremadura) vector map has a scale of 1:25 000 and is an official cartographic source appropriate for the description of the vegetation categories occurring in the study area. As in the previous case, only the vegetation categories present in the study area in considerable proportions were analyzed.

Finally, an ad hoc map was used with vegetation categories grouped according to their hydrological properties in Fragoso-Campón et al. (2021). This map is also in raster format with 10-m resolution that allows distinguishing even between deciduous and evergreen trees, a key aspect in the study of vegetation performance by season.

2.5 Space–time cube analysis

The spatial–temporal relationships between the performance of the SPEI and the vegetation indices were analyzed to verify their spatial pattern and the degree of importance of the vegetation indices in the variation in the SPEI index.

First, to analyze data distributions and patterns in the context of both space and time, spatial–temporal cubes was constructed to analyze the possible clusters with the same temporal variations of all the indices. Then, we performed

partitions of time series, stored in the space–time cubes, based on the similarity of time series characteristics. The clusters were calculated separately for each studied index tending to increase and decrease at the same time and then merged to analyze the locations with the same temporal pattern.

Second, a forest-based forecast analysis, using the random forest algorithm, was performed to analyze whether temporal variations in vegetation indices could explain the performance of the SPEI index. Therefore, SPEI was chosen as the predictor variable, and all vegetation indices were chosen as explanatory variables. The forest regression model was trained using 100 trees and one-fourth of the number of time steps as time windows on each location of the space–time cube. The fit of the predicted model with the time series was further measured with the forecast root mean square error (RMSE) (Eq. 1).

$$\text{Forecast RMSE} = \sqrt{\frac{\sum_{t=1}^T (c_t - r_t)^2}{T}} \quad (1)$$

where T is the number of time steps, c_t is the value of the forecast model, and r_t is the raw value of the time series at time t .

This analysis also involved a study of the lagged effects between the vegetation indices and the SPEI and the importance of the explanatory variables, according to each time lag. Each vegetation index was converted into time lagged predictor within each training time window of the forest model. This allowed estimating any lagged effects between the explanatory variables and SPEI.

3 Results

According to the decay and rise of the time series from March 2005 to March 2006 shown in Fig. 3, there is a similarity of trends between the SPEI index and the vegetation indices.

According to the classification of Zhang et al. (2023), Fig. 3 shows that severe drought was concentrated in summer and autumn, which was higher in the latter season. In the summer and winter seasons, the number of locations and periods with drought were considerable, but their intensity was classified within the light and moderate intervals.

3.1 Index correlations

Figure 4a shows the correlations between the time series. According to ESA_WCM vegetation categories, grassland obtained the highest Pearson correlations values in all the indices, with the FAPAR, LAI and NDVI having the highest correlation with the SPEI index. Furthermore, the highest correlations occurred mainly in autumn, which is

Fig. 3 Average time series and drought severity by season

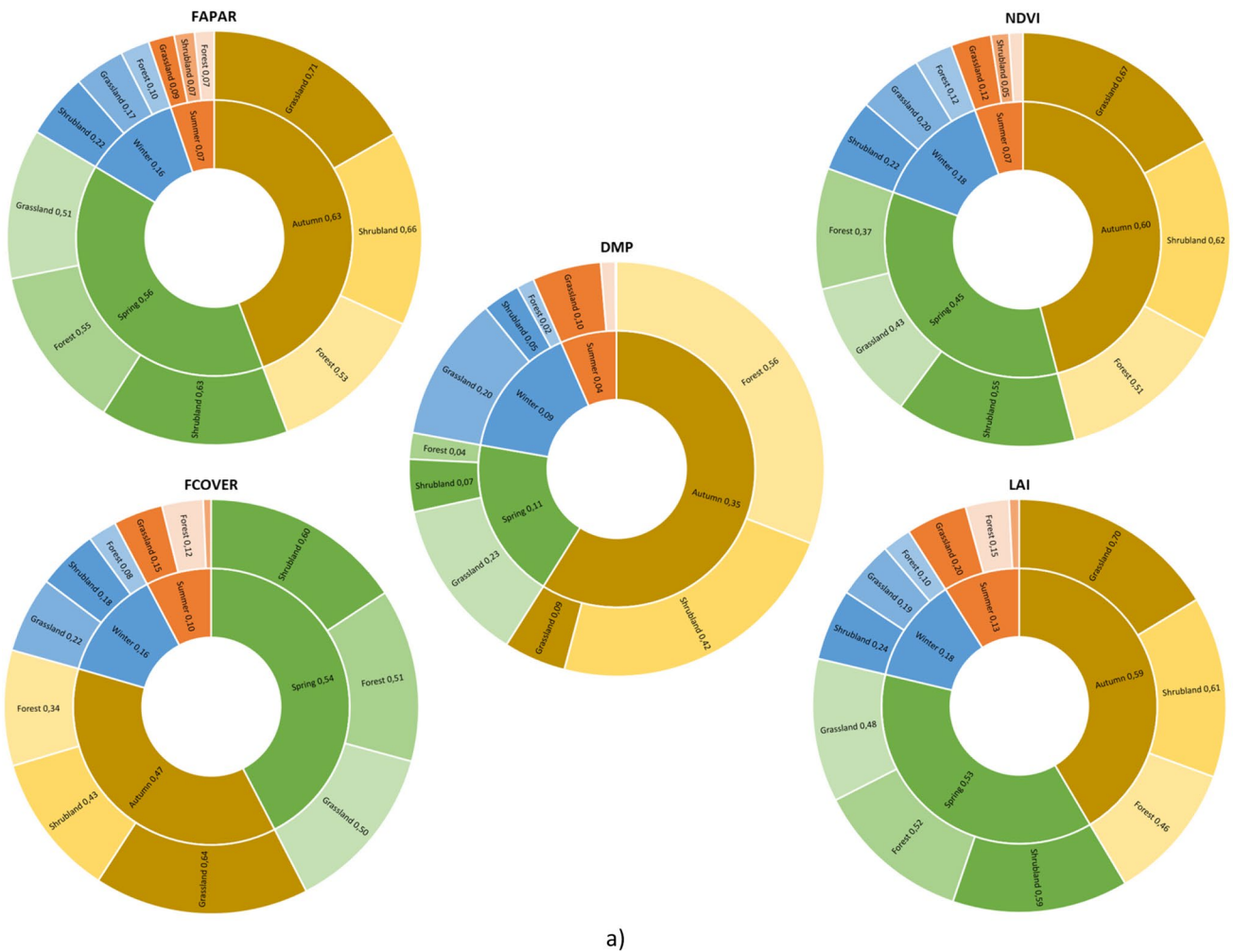
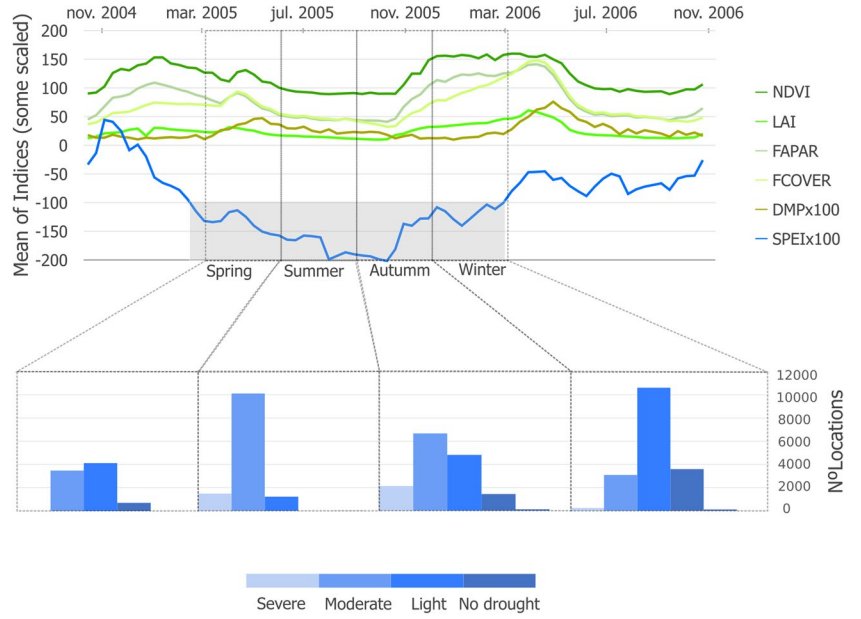


Fig. 4 Pearson correlation values between indices for the (a) ESA_WCM map, (b) FME map, (c) ad hoc map

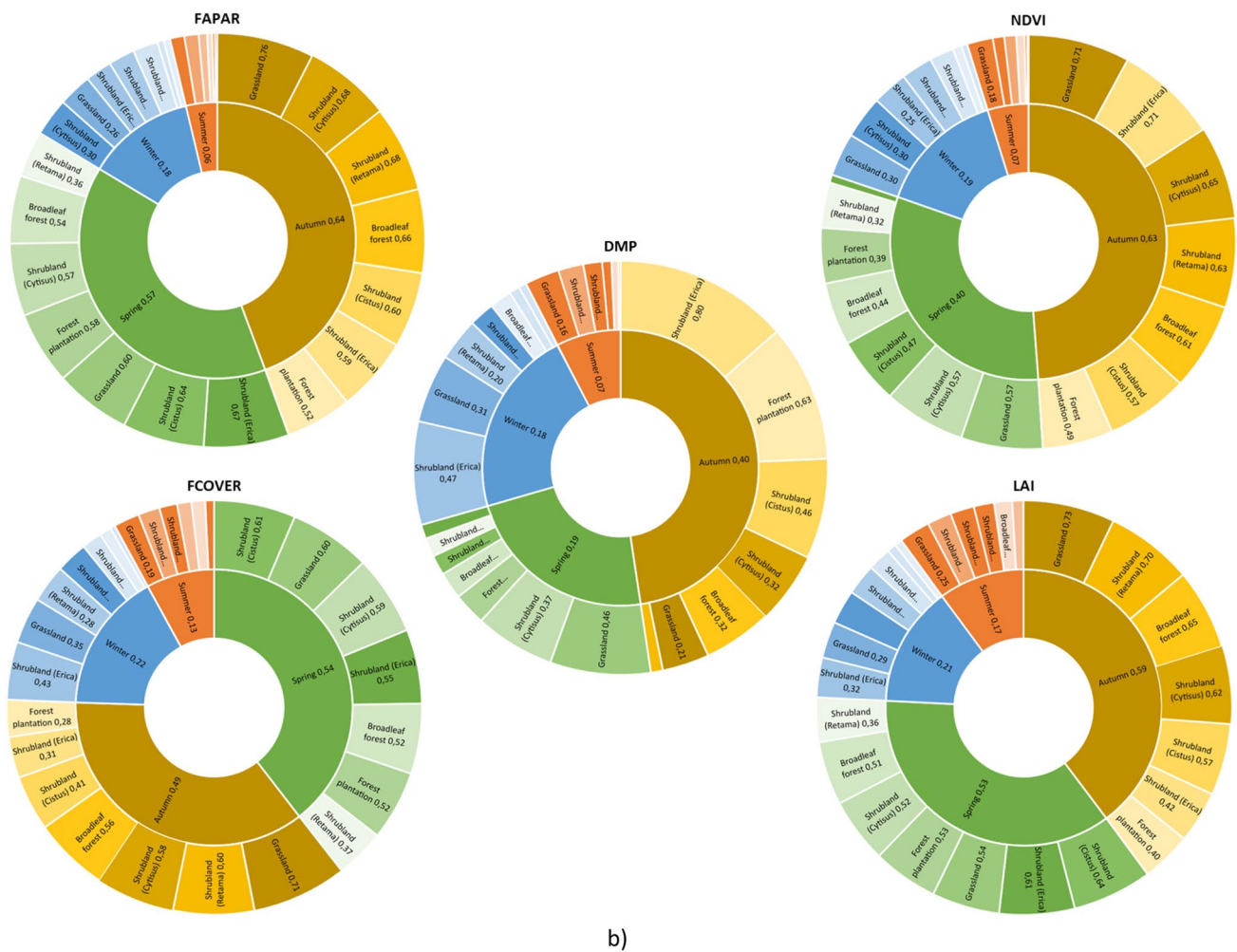


Fig. 4 (continued)

when drought severity was greatest, but slight correlations were also found in spring. In contrast, the DMP index had extremely low correlations in any season of the year.

Regarding the Pearson correlation values for the FME vegetation categories (Fig. 4b), once again, autumn had the highest correlations, especially for FAPAR, LAI and NDVI. This time, since there is higher discrimination of vegetation categories, in addition to grasslands, good results were also obtained for Shrubland (Retama) but only in autumn, since in spring correlations are very low for all the indices in that category. As in the previous map, the DMP index obtained particularly low correlations in these two categories.

Finally, Fig. 4c shows the ad hoc map categories, and the results are more detailed and lead to better interpretations. The same seasonal trends can be observed in the best-correlation seasons and indices. However, in addition to grasslands, high correlations were also found for dehesas, which are very open woodlands with a large amount of grass between them. Additionally, when distinguishing between

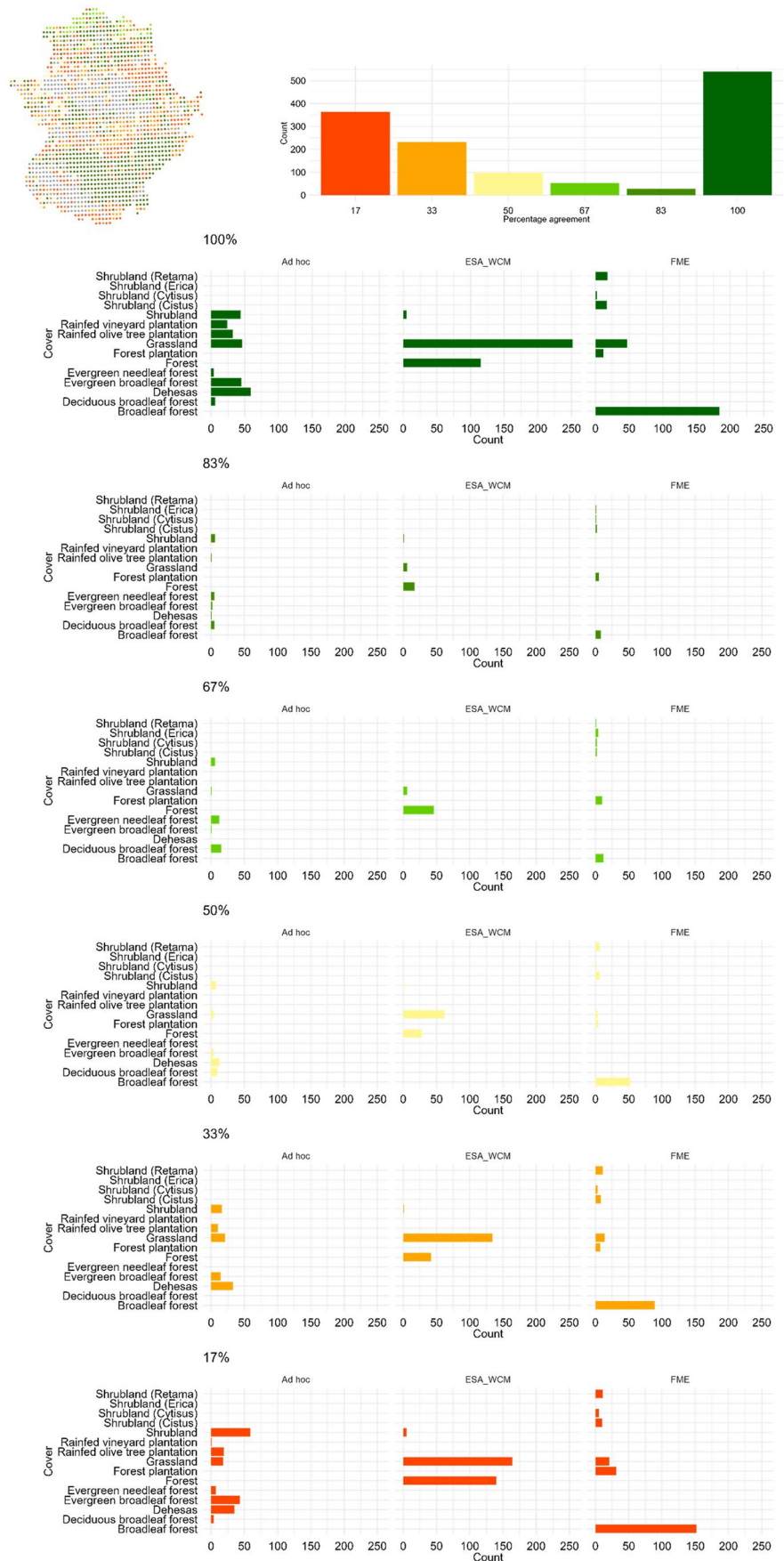
evergreen and deciduous trees, the correlations in autumn are completely opposite when leaves are present and absent. This is the case for evergreen and deciduous hardwood forests. Additionally, the high correlation value for deciduous hardwood forests with the DMP is remarkable, which is also totally opposite to the correlation of the rest of the vegetation indices.

3.2 Space-time cube analysis

Figure 4 shows that in more than 500 locations (dark green), all the studied indices have a similar performance (they were classified within the same cluster). In addition, most of the locations seem to be clustered very close together in specific areas, especially in the south and southeast of the region.

In contrast, more than 300 studied locations coincided in only 17% of the indices in terms of similarity of time series performance. In this case, there is considerably more

Fig. 5 Spatial analysis. Agreement of time series and vegetation types for the ESA_WCM map, FME vegetation map, and ad hoc map



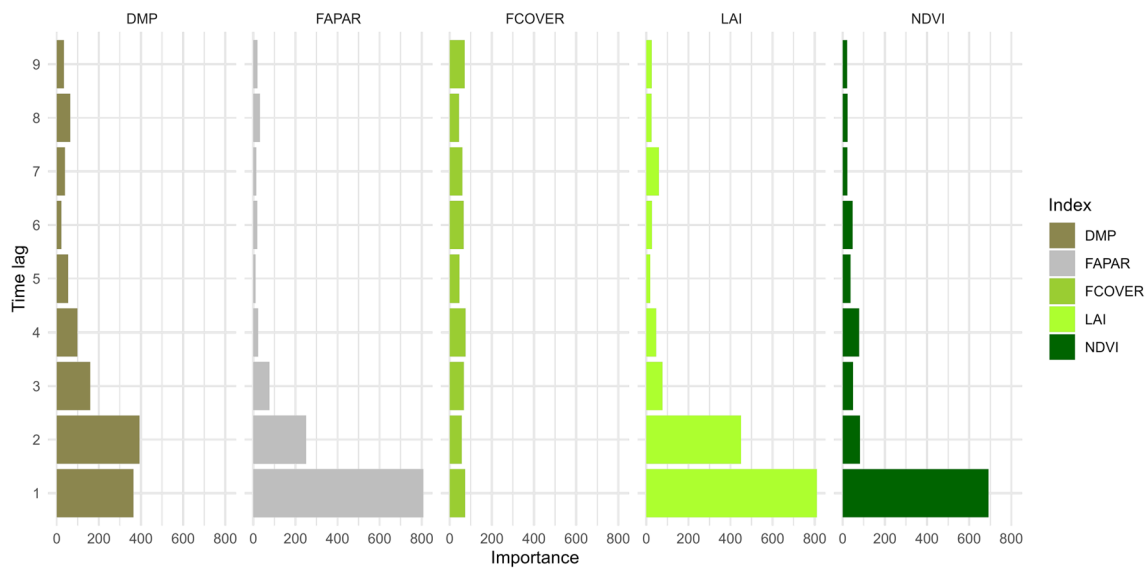


Fig. 6 Importance of variables according to time lags

severe droughts correspond to long SPEI time scales. This 9-month time scale was found by Zhang et al. (2017) to be the most sensitive to vegetation where grasslands are the more dominant cover.

As shown in Fig. 2, in both spring and autumn, the lines representing the average time trend of each index have a notable geometric similarity. This occurs if we compare the SPEI index with the FAPAR, NDVI, and FCOVER indices, and in contrast, we can see that the DMP index does not have this geometric similarity. These similarities are demonstrated by the generally better correlations of the autumn and spring seasons with almost all types of vegetation. This better correlation, especially in autumn, is closely linked to the fact that drought was most severe in this season than in the rest of the year. As is normal, the trends of the vegetation indices decrease in spring and increase in autumn, and we analyzed the degree of similarity of this decrease or increase with that of the drought index. Analyzing Fig. 2 again, it can be seen that when there is no drought (in autumn 2004 or spring 2006), the trend of the SPEI index has no relationship with that of the rest of the vegetation indices.

Regarding the vegetation indices, one of the most strongly correlated with the SPEI is the NDVI. In this context, Jalayer et al. (2023) presented an index closely related to the NDVI and obtained very low Pearson correlation values with the SPEI (0.258 with SPEI at a 6-month time scale). Rhee et al. (2010) used the scaled drought condition index (SDCI), which was also calculated from the NDVI, and obtained Pearson correlation values with a 6-month SPI of approximately 0.70 for an arid region in the month of May and for the grassland category. Considering that our study area also belongs to an arid climate, their results are similar, although slightly lower, to those obtained in this work for grasslands,

especially those categorized by the FME. The difference could be because their vegetation categories also included pasture hay and cultivated crops. In addition, those authors only analyzed 1 month of the whole spring period, and they used the SPI, which does not include the evapotranspiration effect.

Our findings show that LAI has the best correlations with SPEI in most of the categories and mainly in autumn. The effects of drought on the LAI were also analyzed by Bai et al. (2023), and their conclusions confirm our results: the intensity of drought occurrence in autumn has a very high influence on the LAI. In general terms, Kim et al. (2017) obtained good correlations between the LAI and drought (they used a 9-month time scale SPI) based on the idea that LAI values decreased under water stress conditions.

Additionally, the FAPAR index has also been correlated with SPEI in some studies. In this sense, our results were confirmed by Rossi et al. (2008), also working in Spain, who found that FAPAR anomalies seem to be more correlated with precipitation anomalies than NDVI anomalies over a wider range of land cover types, but they recommended that the study should be performed seasonally, as in our case. The European Drought Observatory (European Commission 2019) also recommends the use of the “FAPAR anomaly” as an indicator for the SPEI.

In contrast, the worst results in almost all vegetation types were obtained by the DMP index. In this sense, Smets et al. (2019) confirmed that “Some potentially important factors, such as drought stress, nutrient deficiencies, pests and plant diseases, are omitted in the DMP product... On the other hand, it might be argued that the adverse effects of drought, diseases and shortages of nutrients are manifested (sooner or later) via the RS-derived FAPAR. The DMP

algorithm does not include a water stress factor to account for short-term drought stresses. In drought sensitive vegetation types, this can lead to an overestimation of the actual plant productivity.”

The best vegetation type in terms of correlation was grassland in all studied maps. High evapotranspiration rates or reduced growing seasons caused by increased summer

drought have an unfavorable impact on pasture growth (Rubio and Roig 2017), making it highly vulnerable to drought, especially in warmer climates, as confirmed in Zhang et al. (2021).

This drought impact on vegetation activity in the Mediterranean region has been assessed by Gouveia et al. (2017), who also applied a cluster analysis with the NDVI quantifying drought severity and using the SPEI, and they performed

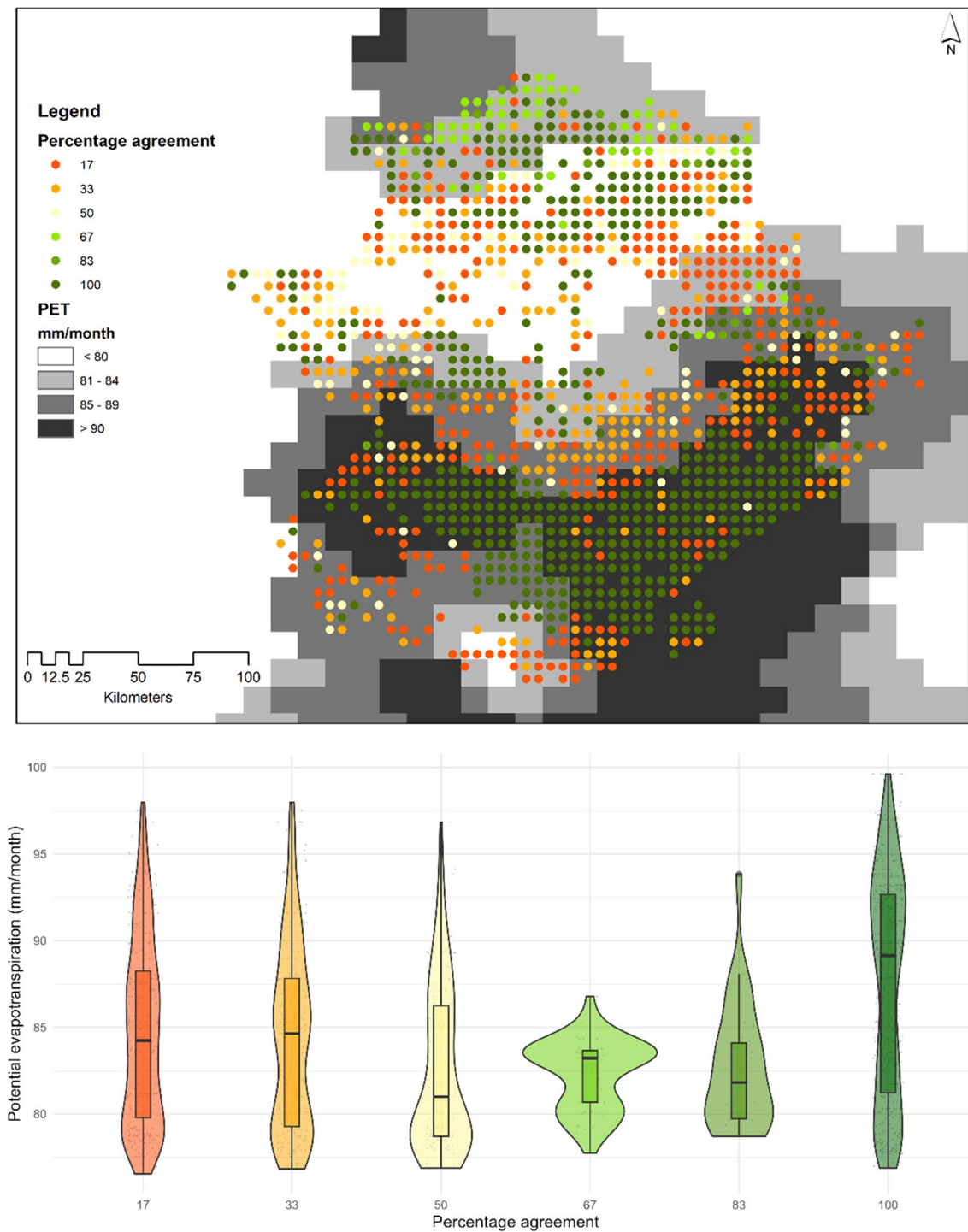


Fig. 7 Potential evapotranspiration of the time series clusters

the correlations by season, although they used only data from one representative month of each season. Our results are consistent with theirs, as they found a good correlation in spring for the vegetation type grouped as Oceanic Mediterranean (OM), which is type that includes our study area. However, their study was not as detailed as ours, as we were able to distinguish the correlation of the NDVI with and other indices for up to 12 vegetation categories (at the ad hoc map).

Regarding the spatiotemporal analysis, Jalayer et al. (2023) also performed a spatiotemporal study of some indices but did not compare the trends and groupings of all of them at the same time in space. In turn, Khoshnazar et al. (2023) performed a cluster analysis for drought data, but they did so not for the time series but for the spatial vulnerability to drought.

As climate change is modifying precipitation and evapotranspiration patterns, droughts will be increasingly severe and frequent throughout the world, especially in the study area due to its aridity and vulnerability. Based on the prediction map of potential evapotranspiration in a historical scenario of the National Plan for Adaptation to Climate Change (PNACC), it can be observed in Fig. 7 that the areas of the region with the highest volume of evapotranspiration are in the cluster in which all the locations studied behave in the same way in terms of vegetation indices and SPEI. These locations with the same performance have a mean potential evapotranspiration value of 87.43 mm/month, while the average for the country is 76.77 mm/month.

5 Conclusions

In this work, we performed a detailed study of the correlations between the SPEI meteorological index, and some vegetation indices provided by the Copernicus Global Land Service program during a prolonged drought episode in the Extremadura region, Spain.

The indices with the highest correlation with the SPEI were the FAPAR, LAI, and NDVI. Since the indices used are freely available and come from a reliable source with good resolution and continental coverage, they are candidates as drought predictors if the SPEI values are not available in the study area.

The correlations were studied by season and according to the vegetation categories classified according to three different cartographies. The results show that grasslands have the highest similarity of performance between all the studied indices. In this sense, the importance of the cartography used is clear, since the greater the detail, the more detailed the vegetation behavior in the face of drought.

For the seasons of the year, the highest correlation was found in autumn and spring. In the analyzed period, drought was the most severe in autumn. In addition, drought has the

greatest effects during vegetation growth and decay, since once the maximum senescence or decay is reached, the climatological variations do not affect the plants.

The results of the spatiotemporal study are consistent with those of the correlation study, since grasslands were found to behave the most consistently temporally.

In addition, the location with coincidence in behavior was located in an area with a prediction of very high evapotranspiration values according to predictive models of climate change.

The major significance of the outcomes of this study reveals the agreement in the spatiotemporal behavior of the indices during the drought period studied also reflects well the vulnerability to drought, therefore, the behavior of the vegetation indices can be used a predictor of drought events.

Supplementary Information The online version contains supplementary material available at <https://doi.org/10.1007/s00704-024-04846-5>.

Author contribution E.Q. performed the Conceptualization, Methodology, Resources, Software, Writing - Original Draft, Writing - Review & Editing, Supervision.

L.F.C. performed Software, Formal analysis, Investigation, Writing - Original Draft, Writing - Review & Editing.

Funding Open Access funding provided thanks to the CRUE-CSIC agreement with Springer Nature. This research was funded by the Earth Observation Data Centre for Water Resources Monitoring (OpenEO Platform Research Grants 2022–2022/00483/001).

We acknowledge Euro-CORDEX for the downloadable data in the viewer developed in the framework of the PNACC and the LIFE SHARA project “Awareness and Knowledge for Climate Change Adaptation.”

We are also grateful for the rest of the free open data used in this study and their corresponding issuing agencies.

Data availability The data during the current study are publicly available in: <https://monitordesequia.csic.es/monitor/?lang=es#index=spei#months=1#week=2#month=9#year=2023> and <https://land.copernicus.eu/global/products>.

Declarations

Ethical approval The authors declare that the manuscript is original and has not been published in any journal.

Consent to participate Not applicable.

Consent for publication The authors declare their consent to publication of the manuscript in “Theoretical and Applied Climatology” journal.

Competing interests The authors declare no competing interests.

Open Access This article is licensed under a Creative Commons Attribution 4.0 International License, which permits use, sharing, adaptation, distribution and reproduction in any medium or format, as long as you give appropriate credit to the original author(s) and the source, provide a link to the Creative Commons licence, and indicate if changes were made. The images or other third party material in this article are included in the article’s Creative Commons licence, unless indicated

otherwise in a credit line to the material. If material is not included in the article's Creative Commons licence and your intended use is not permitted by statutory regulation or exceeds the permitted use, you will need to obtain permission directly from the copyright holder. To view a copy of this licence, visit <http://creativecommons.org/licenses/by/4.0/>.

References

- Abdourahamane ZS, Garba I, Boukary AG, Mirzabaev A (2022) Spatiotemporal characterization of agricultural drought in the Sahel region using a composite drought index. *J Arid Environ* 204:104789. <https://doi.org/10.1016/j.jaridenv.2022.104789>
- Alkaraki KF, Hazaymeh K (2023) A comprehensive remote sensing-based Agriculture Drought Condition Indicator (CADCI) using machine learning. *Environ Chall* 11:100699. <https://doi.org/10.1016/j.envc.2023.100699>
- American Meteorological Society (1997) Meteorological drought-policy statement. *Bull Am Meteorol Soc* 78:847–849
- Bai Y, Liu M, Guo Q, Wu G, Wang W, Li S (2023) Diverse responses of gross primary production and leaf area index to drought on the Mongolian Plateau. *Sci Total Environ* 902:166507. <https://doi.org/10.1016/j.scitotenv.2023.166507>
- Beguiría S, Vicente-Serrano SM, Reig F, Latorre B (2014) Standardized precipitation evapotranspiration index (SPEI) revisited: parameter fitting, evapotranspiration models, tools, datasets and drought monitoring. *Int J Climatol* 34:3001–3023. <https://doi.org/10.1002/joc.3887>
- Cai S, Zuo D, Wang H, Xu Z, Wang G, Yang H (2023) Assessment of agricultural drought based on multi-source remote sensing data in a major grain producing area of Northwest China. *Agric Water Manag* 278:108142. <https://doi.org/10.1016/j.agwat.2023.108142>
- Christian JJ et al (2021) Global distribution, trends, and drivers of flash drought occurrence. *Nat Commun* 12:6330. <https://doi.org/10.1038/s41467-021-26692-z>
- Delegido J, Verrelst J, Rivera JP, Ruiz-Verdú A, Moreno J (2015) Brown and green LAI mapping through spectral indices. *Int J Appl Earth Obs Geoinf* 35:350–358. <https://doi.org/10.1016/j.jag.2014.10.001>
- Devesa Alcaraz JA (1995) *Vegetación y flora de Extremadura*. Universitas Editorial, Badajoz
- European Commission (2019) FAPAR Anomaly
- European Commission (2023) EDO - European Drought Observatory. <https://edo.jrc.ec.europa.eu/edo2/php/index.php?id=1000>. Accessed Feb 2023
- Fragoso-Campón L, Quirós E, Gutiérrez Gallego JA (2021) Optimization of land cover mapping through improvements in Sentinel-1 and Sentinel-2 image dimensionality and data mining feature selection for hydrological modeling. *Stochast Environ Res Risk Assess* 35:2493–2519. <https://doi.org/10.1007/s00477-021-02014-z>
- Gobron N et al (2005) The state of vegetation in Europe following the 2003 drought. *Int J Remote Sens* 26:2013–2020. <https://doi.org/10.1080/01431160412331330293>
- Gouveia C, Trigo RM, Beguería S, Vicente-Serrano SM (2017) Drought impacts on vegetation activity in the Mediterranean region: an assessment using remote sensing data and multi-scale drought indicators. *Global Planet Change* 151:15–27. <https://doi.org/10.1016/j.gloplacha.2016.06.011>
- Gu Y, Brown JF, Verdin JP, Wardlow B (2007) A five-year analysis of MODIS NDVI and NDWI for grassland drought assessment over the central Great Plains of the United States. *Geophys Res Lett* 34. <https://doi.org/10.1029/2006GL029127>
- Huete A, Didan K, Miura T, Rodriguez EP, Gao X, Ferreira LG (2002) Overview of the radiometric and biophysical performance of the MODIS vegetation indices. *Remote Sens Environ* 83:195–213. [https://doi.org/10.1016/S0034-4257\(02\)00096-2](https://doi.org/10.1016/S0034-4257(02)00096-2)
- Jalayer S, Sharifi A, Abbasi-Moghadam D, Tariq A, Qin S (2023) Assessment of spatiotemporal characteristic of droughts using in-situ and remote sensing-based drought indices. *IEEE J Sel Top Appl Earth Obs Remote Sens*. <https://doi.org/10.1109/JSTARS.2023.3237380>
- Khoshnazar A, Corzo Perez G, Sajjad M (2023) Characterizing spatial-temporal drought risk heterogeneities: a hazard, vulnerability and resilience-based modeling. *J Hydrol* 619:129321. <https://doi.org/10.1016/j.jhydrol.2023.129321>
- Kim K, Wang M-c, Ranjitar S, Liu S-h, Xu J-c, Zomer RJ (2017) Using leaf area index (LAI) to assess vegetation response to drought in Yunnan province of China. *J Mt Sci* 14:1863–1872. <https://doi.org/10.1007/s11629-016-3971-x>
- Kogan FN (1995a) Application of vegetation index and brightness temperature for drought detection. *Adv Space Res* 15:91–100. [https://doi.org/10.1016/0273-1177\(95\)00079-T](https://doi.org/10.1016/0273-1177(95)00079-T)
- Kogan FN (1995b) Droughts of the late 1980s in the United States as derived from NOAA polar-orbiting satellite data Bulletin of the. *Am Meteorol Soc* 76:655–668. [https://doi.org/10.1175/1520-0477\(1995\)076%3c0655:DOTLIT%3e2.0.CO;2](https://doi.org/10.1175/1520-0477(1995)076%3c0655:DOTLIT%3e2.0.CO;2)
- Kogan FN (1997) Global drought watch from space. *Bull Am Meteorol Soc* 78:621–636
- Liu X, Zhu X, Zhang Q, Yang T, Pan Y, Sun P (2020) A remote sensing and artificial neural network-based integrated agricultural drought index: index development and applications. *CATENA* 186:104394. <https://doi.org/10.1016/j.catena.2019.104394>
- McKee TB, Doesken NJ, Kleist J (1993) The relationship of drought frequency and duration to time scales. In: *Proceedings of the 8th Conference on Applied Climatology*. vol 22. California, pp 179–183
- Monteith JL (1972) Solar radiation and productivity in tropical ecosystems. *J Appl Ecol* 9:747–766. <https://doi.org/10.2307/2401901>
- Orimoloye IR, Belle JA, Ololade OO (2021) Drought disaster monitoring using MODIS derived index for drought years: a space-based information for ecosystems and environmental conservation. *J Environ Manage* 284:112028. <https://doi.org/10.1016/j.jenvman.2021.112028>
- Palmer WC (1965) *Meteorological drought*, vol 30. US Department of Commerce, Weather Bureau
- Potop V (2011) Evolution of drought severity and its impact on corn in the Republic of Moldova. *Theoret Appl Climatol* 105:469–483. <https://doi.org/10.1007/s00704-011-0403-2>
- Reig F, Domínguez F, Vicente-Serrano SM, Beguería S, Latorre B, Luna Y, Morata A (2023) Monitor de sequía meteorológica. <https://monitordesequia.csic.es/monitor/?lang=es#index=spei#months=1#week=1#month=7#year=2023>. Accessed Feb 2023
- Rhee J, Im J, Carbone GJ (2010) Monitoring agricultural drought for arid and humid regions using multi-sensor remote sensing data. *Remote Sens Data Remote Sens Environ* 114:2875–2887. <https://doi.org/10.1016/j.rse.2010.07.005>
- Rossi S, Weissteiner C, Laguardia G, Kurnik B, Robustelli M, Niemeier S, Gobron N (2008) Potential of MERIS FAPAR for drought detection. In: *2nd MERIS/(A) ATSR User Workshop*. Citeseer, pp 22–26
- Rouse JW, Haas RH, Schell JA, Deering DW (1973) Monitoring Vegetation Systems in the Great Plains with ERTS (Earth Resources Technology Satellite). *Proceedings of 3rd Earth Resources Technology Satellite Symposium, Greenbelt, 10-14 December, SP-351*, pp 309–317
- Rubio A, Roig S (2017) Impactos, vulnerabilidad y adaptación al cambio climático en los sistemas extensivos de producción ganadera en España Oficina Española de Cambio Climático Ministerio

- de Agricultura y Pesca, Alimentación y Medio Ambiente, Madrid:24–25
- Shahzad A, Basit A, Umair M, Makanda TA, Khan FU, Siqi S, Jian N (2023) Spatio-temporal variations in trends of vegetation and drought changes in relation to climate variability from 1982–2019 based on remote sensing data from East Asia. *J Int Agric*. <https://doi.org/10.1016/j.jia.2023.04.028>
- Smets B, Lacaze R (2019) Copernicus Global Land Operations “Vegetation and Energy” “CGLOPS-1” vol Issue I1.20
- Smets B, Swinnen E, Van Hoolst R (2019) Copernicus Global Land Operations “Vegetation and Energy” “CGLOPS-1” vol Issue I3.22
- Tian L, Leason ZT, Quiring SM (2020) Developing a hybrid drought index: precipitation evapotranspiration difference condition index. *Climate. Risk Manage* 29:100238. <https://doi.org/10.1016/j.crm.2020.100238>
- Vicente-Serrano SM, Beguería S, López-Moreno JI (2010) A multi-scalar drought index sensitive to global warming: the standardized precipitation evapotranspiration index. *J Clim* 23:1696–1718. <https://doi.org/10.1175/2009JCLI2909.1>
- Vicente-Serrano SM et al (2012) Performance of drought indices for ecological, agricultural, and hydrological applications. *Earth Interactions* 16:1–27. <https://doi.org/10.1175/2012EI000434.1>
- Vicente-Serrano SM et al (2013) Response of vegetation to drought time-scales across global land biomes. *Proc Natl Acad Sci* 110:52–57. <https://doi.org/10.1073/pnas.1207068110>
- Vicente-Serrano SM et al (2019) A high-resolution spatial assessment of the impacts of drought variability on vegetation activity in Spain from 1981 to. *Nat Hazard* 19:1189–1213. <https://doi.org/10.5194/nhess-19-1189-2019>
- Weiss M, Baret F (2016) S2ToolBox Level 2 products: LAI, FAPAR, FCOVER (Versión 1.1)
- Xie F, Fan H (2021) Deriving drought indices from MODIS vegetation indices (NDVI/EVI) and Land Surface Temperature (LST): Is data reconstruction necessary? *Int J Appl Earth Obs Geoinf* 101:102352. <https://doi.org/10.1016/j.jag.2021.102352>
- Yihdego Y, Vaheddoost B, Al-Weshah RA (2019) Drought indices and indicators revisited. *Arab J Geosci* 12:1–12. <https://doi.org/10.1007/s12517-019-4237-z>
- Zanaga D et al (2022) ESA WorldCover 10 m 2021 v200. 10.5281/zenodo.7254221
- Zhang Q, Kong D, Singh VP, Shi P (2017) Response of vegetation to different time-scales drought across China: Spatiotemporal patterns, causes and implications. *Global Planet Chang* 152:1–11. <https://doi.org/10.1016/j.gloplacha.2017.02.008>
- Zhang L, Gao J, Tang Z, Jiao K (2021) Quantifying the ecosystem vulnerability to drought based on data integration and processes coupling. *Agric for Meteorol* 301:108354. <https://doi.org/10.1016/j.agrformet.2021.108354>
- Zhang J, Ding J, Hou X, Wu P (2023) Quantifying drought response sensitivity and spatial and temporal heterogeneity of vegetation in arid and semi-arid regions. *Int J Remote Sens* 44:1665–1683. <https://doi.org/10.1080/01431161.2023.2182651>

Publisher's Note Springer Nature remains neutral with regard to jurisdictional claims in published maps and institutional affiliations.